SIMULATION OF MULTI-SUPPORT AND MULTI-COMPONENT SPATIALLY VARIABLE GROUND MOTIONS

Z. X. Li[1], X. Q. Li[2] , Q.H. Zhao[3]

[1] *Professor, Key Laboratory of Coast Civil Structure Safety of Ministry of Education, Tianjin University, Tianjin 300072, China. E-mail address: zxli@tju.edu.cn*
[2] *PhD student, School of Civil Engineering, Tianjin University, Tianjin 300072, China. E-mail address: lixiaoqiong@tju.edu.cn*
[3] *Professor, Key Laboratory of Coast Civil Structure Safety of Ministry of Education, Tianjin University, Tianjin 300072, China. E-mail address: qzhao@tju.edu.cn*

Abstract

Spatially variable ground motions should be considered during the seismic response analysis of large-span structures. Based on original spectral representation method (SRM), a simulation method is developed with reasonable spectral density function, coherency function and site transfer function considering spatial correlation， for the non-stationary multi-component and multi-support ground motions on both the bedrock and the ground surface of an engineering site, which has varying soil conditions at different structural supports. Two numerical examples are presented to demonstrate the proposed method. Each generated ground motion time history is compatible with the derived power spectral density at a particular point on the site, and any two of the ground motions are compatible with a model coherency function. Results show that amplification and filtering effects on the incident wave from local site conditions lead to obvious changes in the amplitude and frequency components, even much greater than changes caused by wave passage effects and coherency effects under specific site conditions. Hence it's necessary to use non-uniform spatially variable ground motions with rational consideration of local site effects, when choosing the input for seismic analysis of large-span structures. Simulation of multi-support and multi-component ground motions can be simplified to three independent multi-support one-dimensional ground motions, owing to the critical value of coherency functions through numerical method. Therefore, this simulation method offers an effective way for determine seismic input for the seismic response analysis of large-span structures in practice.

Keywords: Spatial variation; synthetic ground motions; Site effect; Multi-support excitation; Power spectral density

1. Introduction

Reasonable definition of earthquake ground motions is crucial to structural response analysis for seismic design. Although there are a large number of recorded earthquake ground motions collected in the past, the site conditions where these earthquakes were recorded may be quite different from those of the structures. In this case, the existing earthquake ground motions cannot fully meet the actual demand, and it is necessary to simulate earthquake ground motions with certain characteristic parameters [1]. The traditional uniform ground motion input method is acceptable in the seismic analysis of small-scale structures. However, for large-span structures, such as bridges, large-span roof and lifeline systems etc., ground motions at different supports during the same earthquake may be different [2], which is called the "spatial effect of earthquake ground motion", including the wave passage effect, the coherency effect, the local site effect and so on. Most of the current earthquake codes suggest using uniform ground motion input method except Eurocode 8 [3], which takes into account the spatial variations of ground motions. However, spatial effect of ground motion has severe threats on large-span structures, which not only leads to analysis error but also underestimates the seismic responses of structures [4]. In summary, multi-support excitation is a more reasonable and practical seismic input mode for large-span structures.

Spatially correlated multi-support ground motions are generally simulated through theoretical or semi-empirical power spectral density function and coherency function. Zerva and Zervas [2] summarized several representative models to simulate the spatial effect of ground motion, but most of these models are derived from the ground motion data collected in plain topography. Based on the assumption that ground motions at different points have the same intensity (power spectral density function or response spectrum), Hao et al. [5] proposed a model to generate spatially correlated multi-support ground motions using an empirical coherency function and the phase lag caused by apparent velocity. The assumption of uniform intensity is acceptable on plains with uniform soil condition, but it is not applicable in a site with varying soil conditions or valley topography. Der Kiureghian [6] proposed a theoretical coherency function, which represents the power spectral density function of ground motion using site transfer function and the white noise spectrum. The corresponding parameters (central frequency and damping ratio) for this model in three typical sites, i.e., stiff site, medium site and soft site were also demonstrated. Although this model takes into account different soil conditions at various points, it estimates the effect of local site conditions too roughly. Deodatis [7] generated a set of sample functions in nonstationary multivariate stochastic process based on spectral representation method, which could simulate ground motions at spatially correlated points with different power spectral density. Similar to Der Kiureghian model, it is a modified power spectral density function obtained by the filtration process of bedrock white noise when propagating the media with different central frequencies and damping ratios, hence it can only roughly estimate the influence of local site.

Based on the spectral representation method, Der Kiureghian model and the discrete-time function proposed by Safak [8], a program is developed and presented in this paper to simulate spatially correlated multi-support nonstationary earthquake acceleration and displacement time histories on both bedrock and site with multi-layer soils. Then, the power spectral density and coherency curve of simulated ground motions are compared with the target curves. Finally, based on the principal axes model of ground motions proposed by Penzien, a method is developed to simulate multi-dimensional ground motions with consideration of the correlation among different components.

2. Synthesis principle of spatially correlated multi-support earthquake ground motions

2.1 Motion model of bedrock

Generally, the distance between epicenter and ground surface is much larger than the size of a structure, so it can be assumed that the ground motion on bedrock is a zero mean stationary stochastic process with the same intensity and frequency component, in which the power spectral density function could be simulated using Clough-Penzien model [9]:

$$S_g(\omega) = |H_g(\omega)|^2 |H_f(\omega)|^2 S_0$$

$$H_g(\omega) = \frac{\omega_g^2 + 2i\xi_g\omega_g\omega}{\omega_g^2 - \omega^2 + 2i\xi_g\omega_g\omega} \qquad H_f(\omega) = \frac{\omega^2}{\omega_f^2 - \omega^2 + 2i\xi_f\omega_f\omega}$$

(1)

where S_0 is the constant power spectral density function of bedrock white noise (the spectral intensity parameter); $H_g(\omega)$ is the Kanai-Tajimi filter function; ω_g and ξ_g are the central frequency and damping ratio, respectively. In order to reduce the exaggerated low-frequency component of ground motions in Kanai-Tajimi power spectral density function, Clough and Penzien added a high-pass filter $H_f(\omega)$ to Kanai-Tajimi model in series, where ω_f and ξ_f are the central frequency and damping ratio of this high-pass filter, respectively.

If only linear elastic response is considered, the auto-spectral density function of each spatially correlated point in a one-dimensional earthquake field comprising n points of the ground surface and the cross power spectral density function between two arbitrary points can be presented as [10]:

$$S_{jj}(\omega) = |H_j(i\omega)|^2 S_g(\omega)$$

$$S_{jk}(i\omega) = H_j(i\omega) H_k^*(i\omega) S_g(\omega) |\gamma_{j'k'}(d_{j'k'}, i\omega)| e^{-i\omega d_{j'k'}\cos\alpha/v_{app}} \qquad j,k = 1,2,...,n$$

(2)

where $H_j(i\omega)$ and $H_k(i\omega)$ are the site transfer function of two arbitrary points j and k on the ground surface, directly reflecting the influence of local site on the wave propagation, and $*$ represents complex conjugate. For the ground motions on bedrock, the site effect of overlaying soil could be ignored, i.e., $H_j(i\omega)=H_k(i\omega)=1$; $|\gamma_{j'k'}(i\omega)|$ is the lagged coherency loss, representing the coherency effect of ground motions on point j' and point k' and varying from 0 to 1. Based on the records of seismic array, many researchers proposed several corresponding coherency function models [5, 15]. $e^{-i\omega d_{j'k'}\cos\alpha/v_{app}}$ is the time lag caused by wave passage effect, where α is the incident angle of incident waves on bedrock and v_{app} is the apparent wave velocity. The stationary stochastic time history of spatial earthquake ground motions on bedrock could be described using the $n \times n$ power spectral density matrix [2]:

$$\mathbf{S}(i\omega) = \begin{bmatrix} S_{11}(\omega) & S_{12}(i\omega) & & S_{1n}(i\omega) \\ S_{21}(i\omega) & S_{22}(\omega) & & S_{2n}(i\omega) \\ & & & \\ S_{n1}(i\omega) & S_{n2}(i\omega) & & S_{nn}(\omega) \end{bmatrix}$$

(3)

where the diagonal elements $S_{jj}(\omega)\,(j=1,2,\ ,n)$ are auto-spectral functions, which are real and nonnegative with respect to the frequency ω. The other elements $S_{jk}(i\omega)\,(j,k=1,2,\ ,n, j\neq k)$ are cross-power spectral functions and the complex functions with respect to frequency ω, and:

$$S_{jk}(i\omega) = S_{jk}^*(-i\omega) \qquad S_{kj}(i\omega) = S_{kj}^*(i\omega)$$

(4)

Therefore, the power spectral density matrix $\mathbf{S}(i\omega)$ is a positive definite Hermite matrix and could be decomposed using Cholesky factorization, that is [5]:

$$\mathbf{S}(i\omega) = \mathbf{L}(i\omega)\left[\mathbf{L}^*(i\omega)\right]^{\mathrm{T}}$$

(5)

where

$$\mathbf{L}(\omega) = \begin{bmatrix} L_{11}(\omega) & & & \\ L_{21}(\omega) & L_{22}(\omega) & & 0 \\ & & & \\ L_{n1}(\omega) & L_{n2}(\omega) & & L_{nn}(\omega) \end{bmatrix}_{n \times n}$$

(6)

3

The spatially varying ground motions on bedrock can be simplified into a one-dimensional stationary stochastic process $U(t)$ with multi-variables:

$$U(t) = \left[u_1(t), u_2(t), u_3(t), \quad , u_n(t) \right] \tag{7}$$

where the zero mean stationary stochastic process $u_j(t) \left(j = 1,2,3 \quad n \right)$ denotes the acceleration time histories at various points [11] and the corresponding power spectral density matrix is $\mathbf{S}(i\omega)$. According to the original spectrum representation method [5], the earthquake ground motion $u_j(t) \left(j = 1,2, \quad ,n \right)$ to be simulated at an arbitrary point could be expressed as:

$$u_j(t) = \sum_{k=1}^{j} \sum_{i=1}^{N} A_{jk}(\omega_i) \cos[\omega_i t + \theta_{jk}(\omega_i) + \varphi_{ki}(\omega_i)] \tag{8}$$

where $A_{jk}(\omega) = \sqrt{4\Delta\omega} \left| L_{jk}(\omega) \right|$ and $\theta_{jk}(\omega) = \tan^{-1} \left(\operatorname{Im} \left[L_{jk}(\omega) \right] \big/ \operatorname{Re} \left[L_{jk}(\omega) \right] \right)$ are the amplitude and phase of the simulated generated acceleration time histories, whose frequency spectrum coincides with the target spectrum in Eq. (2). N is the number of discretized frequency points; ω_u is the upper cut-off frequency, $\Delta\omega = \omega_u / N$ is the frequency increment and $\omega_i = i\Delta\omega$. φ_i is the independent stochastic phase angle between 0 and 2π. The above equation is feasible only if the frequency component greater than the upper cut-off frequency in power spectral density function could be neglected [12], then the cross power spectral density matrix corresponding to this high-frequency component could be assumed to be zero.

Spatially correlated ground motions simulated using the aforementioned method is a stationary stochastic process, but the actual earthquake ground motions have strong non-stationary characteristics. If the phase difference spectrum is unknown, the stationary ground motion model is often multiplied with an envelope function $f(t)$ to achieve the non-stationary process [13], that is:

$$x_j(t) = f(t) \cdot u_j(t) \tag{9}$$

2.2 Motion model of surface

The amplitude of earthquake waves increases significantly when they penetrate the soft soil, which is called site amplification effect and can cause crucial structural damage. Although finite element software can simulate the propagation path of earthquake wave in the soil, a reasonable numerical model will be more applicable in practical projects during analysis on sites with different kinds and thicknesses of soils.

Research on frequency spectrum of earthquake waves during the propagation process is very limited. Based on the theory of seismic wave propagation proposed by Aki, Safak obtained the vertical transfer function of shear wave in horizontal medium layer [8]. For the bedrock overlaid by single-layer soil, the relationship between the arbitrary point j on surface and the corresponding vertical projection point j' on bedrock could be expressed as:

$$H_j(i\omega) = \frac{U_j(i\omega)}{U_{j'}(i\omega)} = \frac{(1 + r_j - i\xi_j) e^{-i\omega\tau_j(1-2i\xi_j)}}{1 + (r_j - i\xi_j) e^{-2i\omega\tau_j(1-2i\xi_j)}} \qquad \left(j = 1,2, \quad ,n \right) \tag{10}$$

where the damping ratio ξ_j denotes the attenuation effect caused by energy dissipation during the propagation process. $\tau_j = h_j / v_j$ is the propagation time of seismic waves from point j to point j'. r_j is the reflection coefficient of the up-going waves within the soil layer, which can be computed using Eq. (11):

$$r_j = \frac{\rho_r v_r - \rho_j v_j}{\rho_r v_r + \rho_j v_j} \tag{11}$$

where $U_j(i\omega)$ and $U_{j'}(i\omega)$ are the Fourier transform of the time histories $u_j(t)$ and $u_{j'}(t)$ on surface point j and bedrock point j', respectively. This transfer function $H_j(i\omega)$ directly represents the relationship of ground motions caused by the filtration and amplification effects between the surface point and the corresponding bedrock point in the same

earthquake. It can be seen that this transfer function is only related to the physical parameters of the local site condition. Safak extended the above formula for single-layer soil and proposed a general transfer function [8] for the site with bedrock overlaid by m-layer soil ($m \geq 2$), which can be used to describe the amplification effect of the arbitrary m-layer soil on the seismic waves transferred from the bedrock to the surface, as shown below:

$$H_{Qm}(i\omega) = \frac{\det\left|\mathbf{I} - \mathbf{\Lambda\Omega}_1\right|}{\det\left|\mathbf{I} - \mathbf{\Lambda\Omega}\right|}(1 + r_m)q^{-\tau_m/T} \qquad\qquad q = e^{i\omega T} \qquad\qquad (12)$$

where $\mathbf{I}$ is the $2m \times 2m$ unit matrix; $\mathbf{\Omega}$ is the $2m \times 2m$ coefficient matrix, which is related to the reflection and penetration coefficient r of every soil layer, and most of the elements are zero including the diagonal elements. $\mathbf{\Omega}_1$ is the matrix obtained after replacing the column vector corresponding to u_1 with $(1,0,0,0,\ldots,0,0,0)^T$ in matrix $\mathbf{\Omega}$. $\mathbf{\Lambda}$ is the $2m \times 2m$ diagonal matrix, in which the diagonal elements are comprised of the filtration coefficient λ caused by the damping of every soil layer, i.e., diag($\mathbf{\Lambda}$)=(λ_m, λ_m, λ_{m-1}, λ_{m-1},…, λ_2, λ_2, λ_1, λ_1), and:

$$\lambda_i = \frac{1 - \alpha_i}{2} \cdot \frac{1 + q^{-1}}{1 - \alpha q^{-1}} \qquad\qquad \alpha_i = \frac{1 - \sqrt{1 - \cos^2\theta_i}}{\cos\theta_i} \qquad\qquad \theta_i = \ln 2 \cdot \frac{4\xi_i T}{\tau_i} \qquad\qquad (13)$$

where T is the time interval; ξ_i is the damping ratio. By programming using the above parameters and equations and inputting the corresponding soil parameters, the transfer function $H_{Qm}(i\omega)$ caused by the filtration of multi-layer soil could be solved. In practical applications, the required physical parameters can be obtained through actual measurements and recorded ground motions. Substituting Eq. (10) or Eq. (12) to Eq. (2) and considering the multi-support ground motion model proposed in section 1.1, the spatially correlated multi-support ground motions could be obtained with consideration of the local site effect.

3. Synthesis of spatially correlated multi-support earthquake ground motions

3.1 Site survey

The site condition of a bridge in the mountain area is shown in Fig.1. Three supporting points are selected along the wave propagation direction with a distance interval equal to 200m. The corresponding physical parameters of soils are presented in Table 1. Parameters of the horizontal earthquake ground motion are shown below:

$$\omega_g = 10\pi\,\text{rad/s},\ \xi_g = 0.6,\ \omega_f = 0.5\pi\,\text{rad/s},\ \xi_f = 0.6,\ S_0 = 0.0034\,\text{m}^2/\text{s}^2 \qquad\qquad (14)$$

which corresponds to an earthquake time history with a time duration of 20s [14] (PGA = 0.2g, PGD = 0.082m).
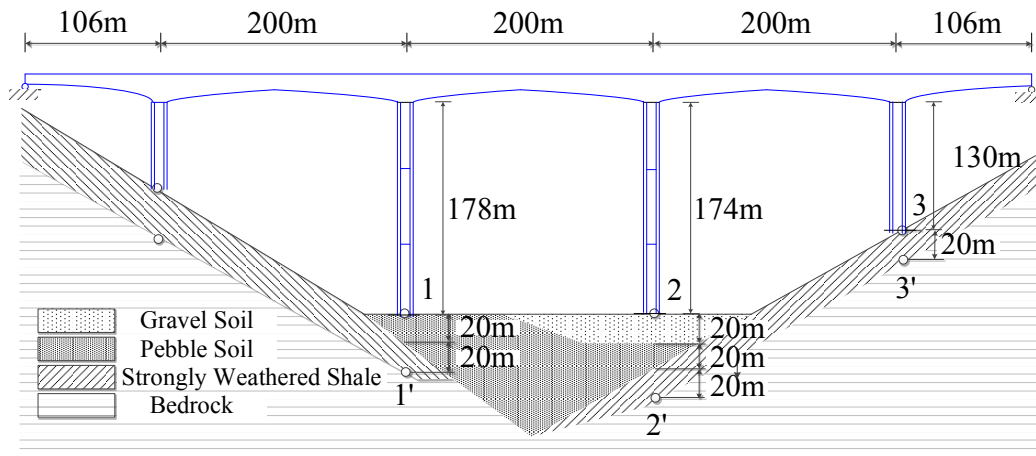

Fig. 1 – A canyon site with multiple soil layers

Table 1 – Characteristic parameters of the soil

Soil Type	Density/ρ(g•cm^{-3})	Shear wave velocity/v(m/s)	Damping ratio/ξ
Bedrock	2.8	1500	0.05
Strongly weathered shale soil	2.7	700	0.05
Pebble soil	2.1	500	0.10
Gravel soil	1.8	400	0.10

The Sobczyk model [15] is used to consider the coherency effect. For the ground motions of two arbitrary points j' and k' on bedrock, the coherency function could be expressed as:

$$\gamma_{j'k'}(i\omega) = \left|\gamma_{j'k'}(i\omega)\right| e^{-i\omega d_{j'k'}\cos\alpha/v_{app}} = e^{-\beta\omega d_{j'k'}^2/v_{app}} \cdot e^{-i\omega d_{j'k'}\cos\alpha/v_{app}} \tag{15}$$

where the coherency coefficient β is 0.0005. Assuming the incident angle α of the incident wave on bedrock is 60°, the apparent velocity v_{app} can be taken as 1768m/s based on the characteristics of bedrock and the specified incident angle. As shown in Figure 1, $d_{1'2'} = d_{2'3'} = 200\text{m}$. The upper cut-off frequency ω_u in the simulation process is assigned to be 50 rad/s; the time duration of the ground motion is 20s and the time step dt is 0.01s. In order to analyze the site effect on the characteristics of ground motion, properties of ground motions on bedrock points (1', 2', and 3') are compared with those obtained on surface points (1, 2, and 3).

3.2 Synthetic earthquake ground motions generated on bedrock points

Three horizontal earthquake acceleration time histories are generated on bedrock points and shown in Fig.2(a). The corresponding displacement time histories after two integral transformation are presented in Fig.2(b). The PGAs of the simulated earthquake time histories are 2.45m/s^2, 2.47m/s^2 and 2.36m/s^2, respectively, and the PGDs are 0.102m, 0.097m, and 0.104m, respectively. These parameters are close to the theoretical characteristics of the selected ground motion (PGA = 0.2g, PGD = 0.082m). Then, using the periodogram averaging method, the auto-power spectral density of three simulated ground motions and cross-power spectral density are computed and compared with the target power spectral density function, as illustrated in Fig.3-5.
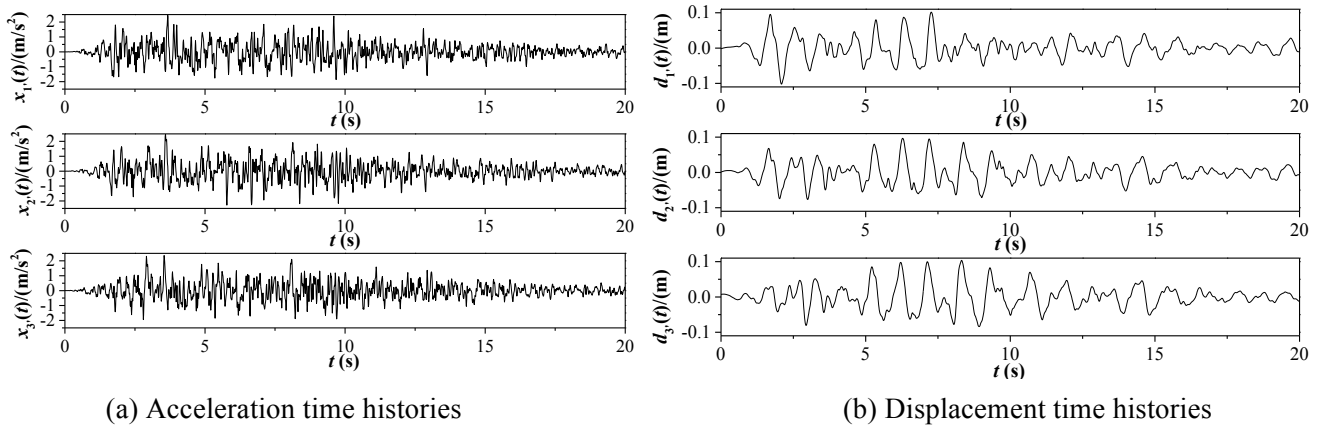

(a) Acceleration time histories   (b) Displacement time histories

Fig.2 Simulated non-stationary ground motions (on bedrock)

(a) x_1,   (b) x_2,   (c) x_3,
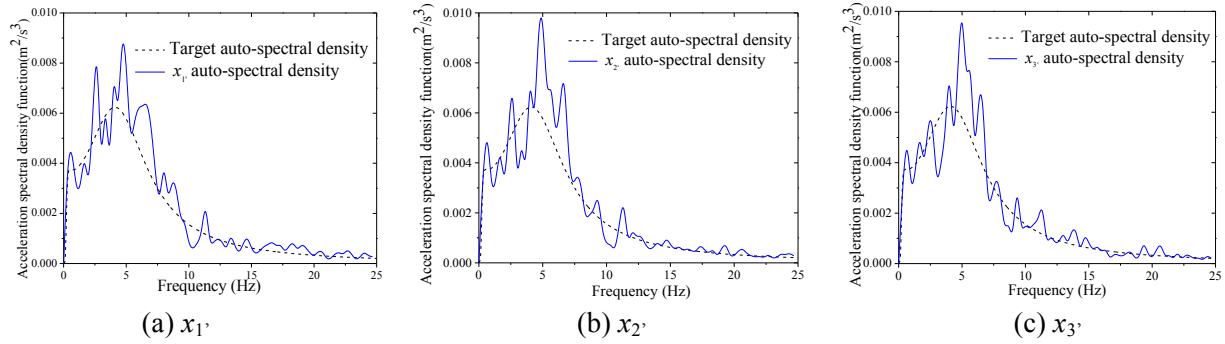
Fig.3 Auto-spectral density functions of simulated ground motions

(a) x_1, x_2,   (b) x_2, x_3,   (c) x_1, x_3,
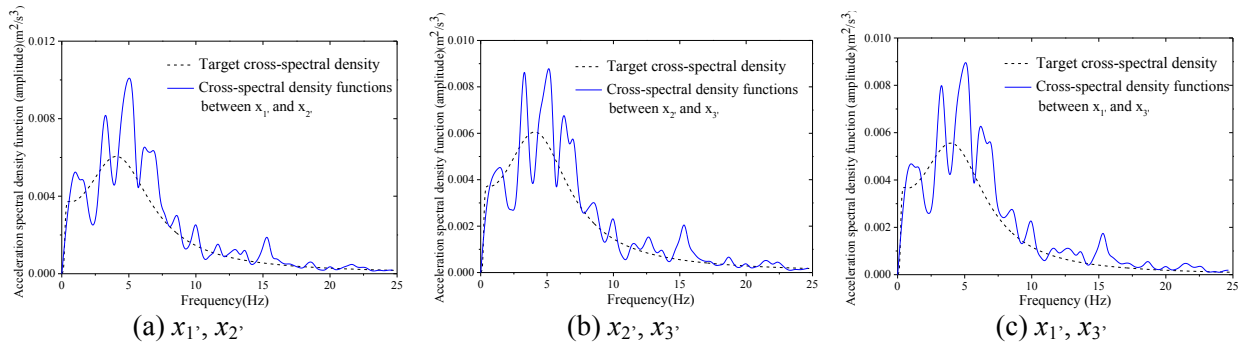
Fig.4 Comparison of cross-spectral functions between generated accelerations with model (amplitude)
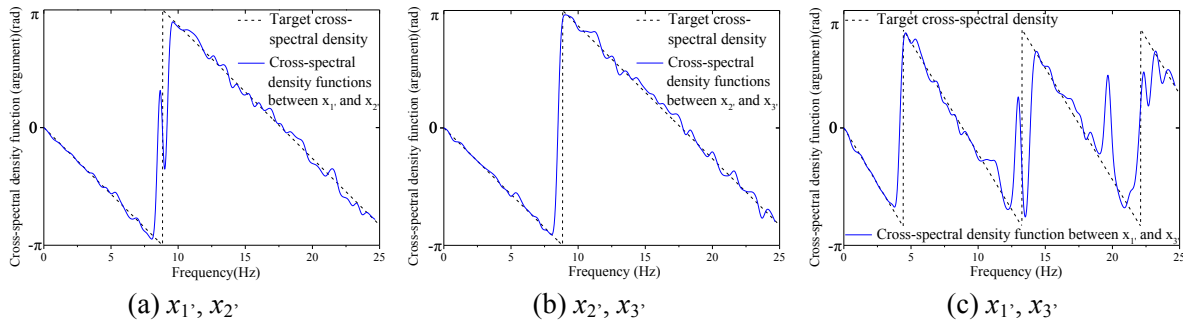

(a) x_1, x_2,   (b) x_2, x_3,   (c) x_1, x_3,

Fig.5 Comparison of cross-spectral functions between generated accelerations with model (phase)

As can be observed in Figure 3, the auto-spectral functions on bedrock points are in good agreement with the target functions. According to Eq. (2), the cross-spectral function is complex. Therefore, the amplitude and phase angle of cross-spectral functions obtained from the simulated ground motions on bedrock points are compared with those of target cross-spectral functions in Fig.4−5, respectively. It can be seen that the simulated values of cross-spectral functions among different bedrock points agree well with the target values.

3.3 Synthetic earthquake ground motions generated on surface points

According to the discrete time-domain method proposed by Safak [8], the horizontal earthquake ground motions on surface points shown in Fig.1 are generated and the corresponding acceleration and displacement time histories are shown in Fig.6. It is noted that the site effect, in a certain way, changes the frequency component of the incident waves and increases the amplitude. However, different site-amplification effects can be found for different penetration paths. As shown in Fig.6, the PGAs of the simulated earthquake time histories are 4.32m/s^2, 4.57m/s^2 and 2.48m/s^2, respectively. The PGDs are 0.188m, 0.160m and 0.092m, respectively. Compared with the ground motions simulated on bedrock points, the acceleration amplification effect on Point 2 is most obvious. However the peak ground displacement doesn't correspond to the largest displacement amplification effect, because the acceleration amplification effect is mainly related to the resonance caused by the approximation

between the soil natrual frequency and the central frequency of the ground motion, while the displacement amplification effect of ground motion is significantly affected by the soil stiffness [15]. In general, the softer the soil, the larger the peak displacement, but the corresponding relationship is not obvious.
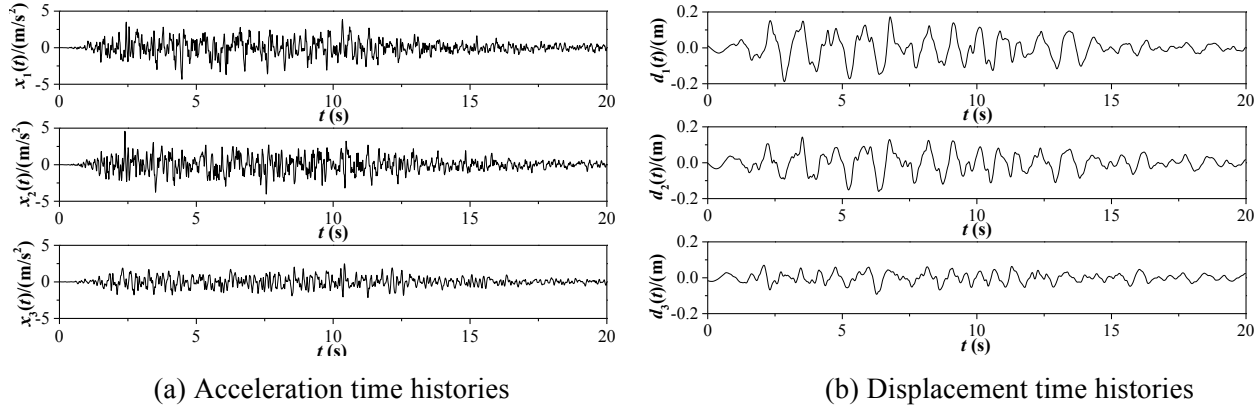

(a) Acceleration time histories   (b) Displacement time histories

Fig.6 Simulated non-stationary ground motions (on surface)

Fig.7 presents the comparison of cross-spectral functions between the simulated ground motions and the theoretical values. It can be seen that they are in relatively good agreement with each other in frequency component. However, the filtering effect of soil changes the distribution of earthquake energy in frequency bands: on Point 1 the curve moves to low-frequency component because of the overlaid pebble soil, thereby deviating from the target cross-spectral functions; on Point 2, distribution of peak frequency has slight oscillations after the ground motion gets filtered by multi-layer soils, but the cross-spectral functions still match well with the target values; the bedrock is only overlaid by a single layer of strongly weathered shale on Point 3, which belongs to hard soil. Compared with the results obtained from Points 1 and 2, the energy distribution on Point 3 is more uniform and there is no obvious predominant period. Hence it is obvious that the characteristics and laws of the simulated synthetic ground motions after filtered by multi-layer soils in this paper basically agree with those from practical experiences [16]. This model could be used for the simulation of synthetic earthquake ground motions in practical site and for the seismic design and analysis of structures.

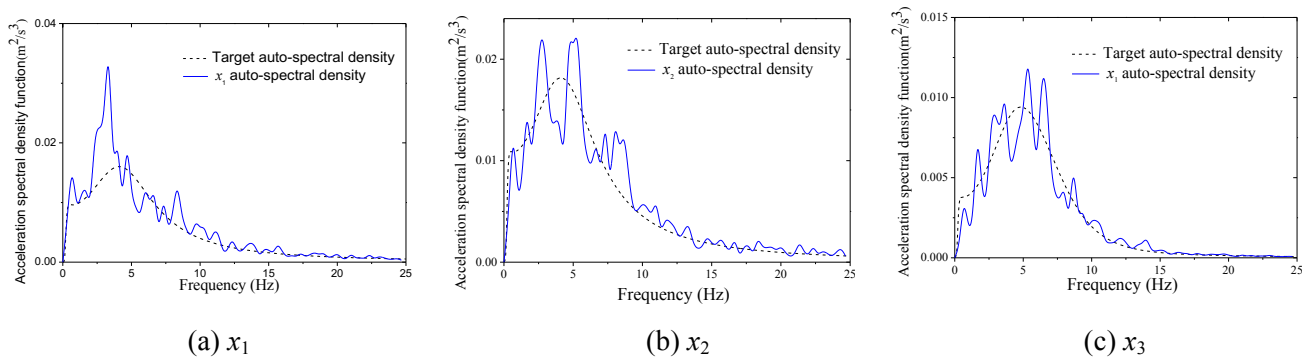(a) x_1 (b) x_2 (c) x_3

Fig.7 Auto-spectral density functions of simulated ground motions

The coherency curves of acceleration time histories generated on surface points are compared with Sobcyzk coherency function in Fig.8. As shown in Fig.8, the coherency loss functions between generated accelerations are consistent with the corresponding Sobcyzk coherency function in the low-frequency range, but the errors in the high-frequency range of lagged coherency loss γ_{12} and γ_{23} as well as the whole range of γ_{13} are relatively large. This is because the correlation between the ground motions on various spatial points remarkably decreases with the increase of distance and frequency. According to the previous studies, the cross correlation function between two arbitrary white noises generally varies from 0.3 to 0.4 [5]. Hence, although the theoretical value of the selected cross correlation function is less than 0.4, the coherency coefficient between two arbitrary time histories simulated in this study is still about 0.4. Therefore, the critical value of coherency coefficient

8

between the simulated earthquake ground motions is between 0.3 and 0.4, resulting in the fact that the corresponding curves do not decrease continuously with the theoretical value, after the high-frequency component of γ_{12} and γ_{23} and most components of γ_{13} fall to around 0.4 in Fig.8.
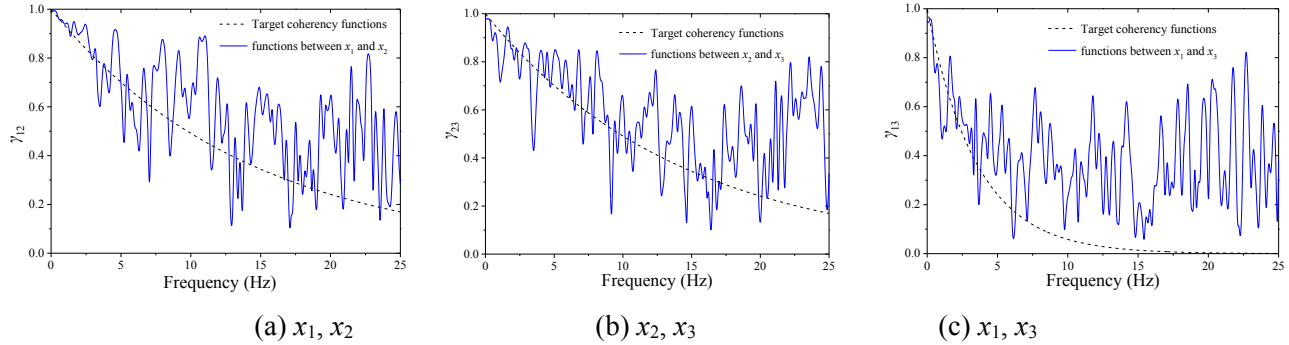

(a) x_1, x_2 (b) x_2, x_3 (c) x_1, x_3

Fig.8 Comparison of coherency loss functions between generated accelerations with model

From Fig.8, it is clear that the influence of site effects on earthquake ground motions is more obvious than the wave passage effects and the coherency effects. In real projects, large-span structures may undergo variations of site characteristics in the longitudinal and the vertical directions, and the amplification and filtration effects of local site conditions on the incident waves should not be neglected. In order to obtain more reasonable results, the earthquake ground motions on different supports should be determined respectively in seismic analysis, and the non-uniform excitations with consideration of local site effects should be adopted as seismic inputs.

4. Synthesis of multi-support and multi-dimensional spatially correlated earthquake ground motions

Unlike uni-axial excitation, the influence of multi-component earthquakes should be considered when structures are subjected to multi-dimensional seismic excitations. Multi-dimensional earthquake ground motions are generally simulated by using the principal axis model proposed by Penzien [17], which assumes that the angle between the maximum principal axis direction and the propagation direction of earthquake is α and the earthquake travels along the longitudinal direction of the structure, as shown in Fig.9(a).

According to Chinese code for seismic design of buildings [18], peak accelerations of multi-dimensional ground motions are generally adjusted by using the following ratio: 1 (horizontal 1): 0.85 (horizontal 2): 0.65(vertical). The power spectral functions of earthquake ground motion accelerations in three principal directions $S_x(\omega):S_y(\omega):S_z(\omega)=$ 1:0.7225:0.4225 and the coherency curve $\rho_{xy}(\omega)$ between the two horizontal components can be expressed as:

$$\rho_{xy}(\omega) = \frac{|(1-a)\sin 2\alpha|}{\sqrt{(a+1)^2 - (1-a)^2 \cos^2 2\alpha}} \qquad a = S_y(\omega)/S_x(\omega) \qquad (16)$$

Likewise, the coherency curves among other components, i.e., $\rho_{yz}(\omega)$ and $\rho_{xz}(\omega)$, could be obtained and presented in Fig.9(b). Assuming that the maximum principal axis direction coincides with the propagation direction of the earthquake motion, i.e., $\alpha=0$, the coherency coefficient among different components at fixed points is zero. The possible maximum coherency coefficient between the horizontal direction x and the vertical direction z is about 0.4. In fact, the cross correlation coefficient between two arbitrary white noises in general varies between 0.3 and 0.4 [5]. Although the coherency between two components of the earthquake ground motion is assumed to be zero, the coherency function between the two components of simulated earthquake ground motion is still above the critical value. In practical applications, ignoring the coherency between various components at the same point and between different components at different points, one-dimensional and multi-support time histories of two horizontal and one vertical earthquake components could be simulated respectively. In this way, simulation of multi-dimensional and multi-support ground motions can be simplified into simulations of three one-dimensional and multi-support ground motions.

9
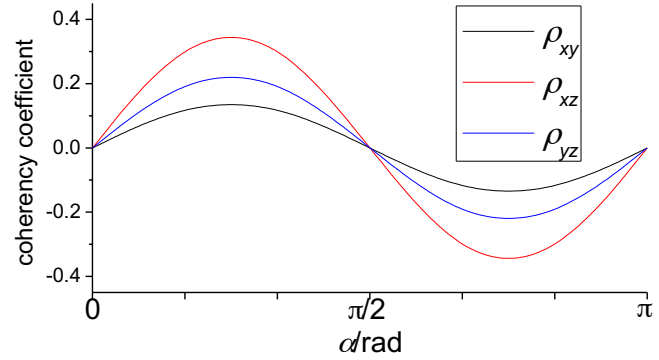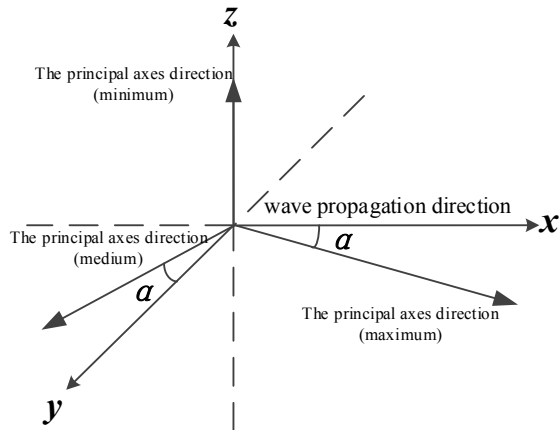
(a) Principle axes model of multi-dimensional motion (b) coherency coefficient curve

Fig.9 Principal axes model of multi-dimensional motion

Take Point 1' on the bedrock in Fig.1 for example. The ratio of peak acceleration among three components is assigned to be 1:0.85:0.65 [18] and the identical coherency model and envelope function are used in both the horizontal and the vertical ground motions. Three principal axes components of simulated earthquake acceleration time histories on Point 1' are shown in Fig.10. The comparisons of power spectral function between various earthquake components and the target values presented in Fig.11 are in good agreement, indicating that the multi-dimensional synthetic ground motion time histories could be simulated using the aforementioned model and method.
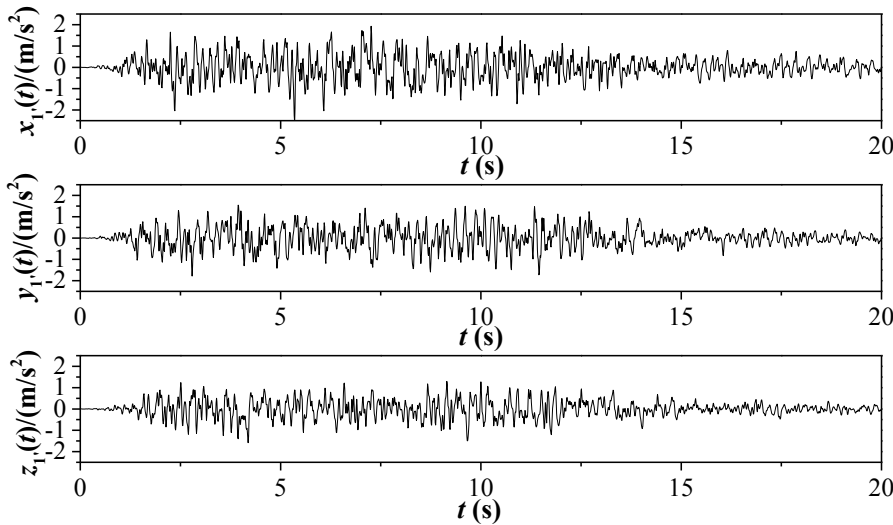

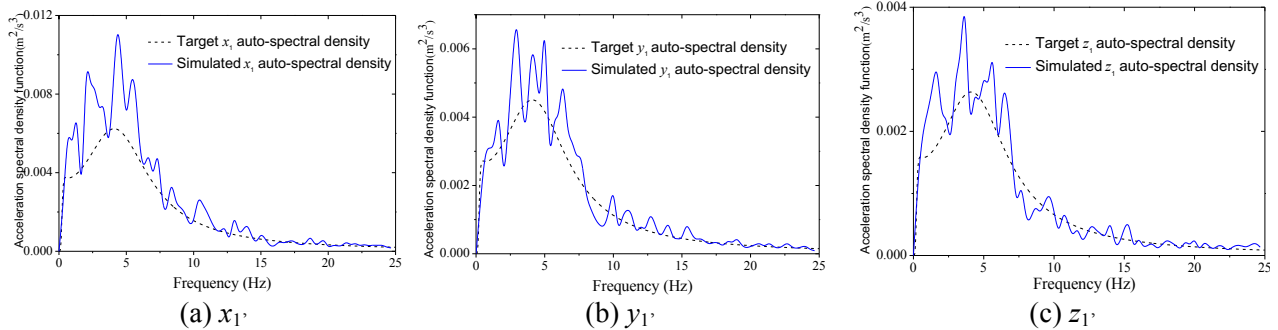Fig.10 Simulated ground motions of a particular point on three dimensions

(a) x_1' (b) y_1' (c) z_1'

Fig.11 Auto-spectral density functions of simulated ground motions

5. Conclusion

Starting with the bedrock white noise spectrum and based on the original spectral representation method, this paper describes the methods to simulate the following ground motions respectively, including: 1) ground motions on bedrock without consideration of site effects; 2) spatially correlated multi-support ground motions on surface considering filtration and amplification of multi-layer soils; 3) multi-dimensional and multi-support synthetic ground motions. Feasibility of the simulation methods is then verified by an example. Based on the obtained results, the following conclusions could be drawn:

(1) The amplification and filtration effects of local site conditions on incident waves significantly change the amplitude and frequency components. On specific site conditions, the local site effect presents more significance than the wave passage effects and the coherency effects. When thesoil properties along the bridge vary obviously or they are approximately uniform but the continuous bridge has a long span,, the spatially variable ground motion model with rational consideration of local site effects should be adopted as excitation inputs.

(2) Compared with some proposed models, discrete time-domain model directly connects the local site conditions and the characteristics of bedrock motion with the ground motion through transfer function, which truly reflects the influence of site amplification effect on shear waves transferred from bedrock to surface, hence it can be applied in the seismic analysis of practical projects.

(3) When using the proposed method to simulate synthetic ground motions, multi-dimensional and multi-support ground motions could be simplified as three independent one-dimensional and multi-support ground motions, owing to the critical value of the coherency function.

(4) The proposed method in this paper could be extended to simulate spatially varied earthquake ground motions on sites where the geometric terrain and the difference of local site conditions need to be considered.

6. Acknowledgements

7. References

[1] Zhang YH, Li QS, Lin JH (2009): Random vibration analysis of large-span structures subjected to spatially varying ground motions. *Soil Dynamics and Earthquake Engineering*, 29, 620-629.

[2] Zerva A, Zervas V (2002): Spatial variation of seismic ground motions: an overview. *American Society of Mechanical Engineers*, 55(3), 271-296.

[3] European Standard EN 1998-2:2005. *Eurocode 8: Design of structures for earthquake resistance, Part2: Bridges*. Brussels: European Committee for Standardization.

[4] Saxena V, Deodatis G, Shinozuka M (2000): Effect of spatial variation of earthquake ground motion on the nonlinear dynamic response of highway bridges. *12th World Conference on Earthquake Engineering*.

[5] Hao H, Oliveira CS, Penzien J (1989): Multiple-station ground motion processing and simulation based on SMART-1 array data. *Nuclear Engineering and Design*, 111(3), 293-310.

[6] Der Kiureghian A (1996): A coherency model for spatially varying ground motions. *Earthquake Engineering and Structural Dynamics*, 25(1), 99-111.

[7] Deodatis G (1996): Simulation of ergodic multivariate stochastic processes. *Journal of Engineering Mechanics*, 122(8), 778-787.

[8] Safak E (1995): Discrete-time analysis of seismic site amplification. *Journal of Engineering Mechanics*, 121(7), 901-809.

[9] Clough RW, Penzien J (1993): *Dynamics of structures*. NewYork: McGraw Hill, Inc.

[10] Hao H, Chouw N (2006): Modelling of earthquake ground motion spatial variation on uneven sites with varying soil conditions, *9th International Symposium on Structural Engineering for Young Experts*, 79-85.

[11] Paola MD, Zingales M (2000): Digital simulation of multivariate earthquake ground motions. *Earthquake Engineering and Structural Dynamics*, 17(2), 1011-1027.

[12] Shinozuka M (1972): Monte Carlo solution of structure dynamics. *Compute Structure*, 2, 855-874.

[13] Huo JR, Hu YX, Feng QM (1991): Study on envelope function of acceleration time history. *Earthquake Engineering and Engineering Vibration*, 11(1), 1-12. [in Chinese]

[14] Bi KM, Hao H (2012): Modelling and simulation of spatially varying earthquake ground motions at sites with varying conditions. *Probabilistic Engineering Mechanics*, 29, 92- 104.

[15] Sobczky K (1991): *Stochastic wave propagation*. Netherlands, Kluwer Academic Publishers.

[16] Li HN (2006): *Earthquake resistant theory of structures to multi-dimensional excitations*. Beijing, Science Press. [in Chinese]

[17] Penzien J, Watabe M (1974): Characteristics of 3-dimensional earthquake ground motions. *Earthquake Engineering and Structural Dynamics*, 3(4), 365-373.

[18] GB50011-2010. *Code for Seismic Design of Buildings*. Beijing, China Architecture & Building Press. [in Chinese]